Acta Mechanica Solida Sinica, Vol. 22, No. 4, August, 2009 ISSN 0894-9166
Published by AMSS Press, Wuhan, China.

FREE VIBRATION ANALYSIS OF ARBITRARY SHAPED PLATES BY BOUNDARY KNOT METHOD**

Jisong Shi **Wen Chen*** **Chanyuan Wang**

(*Center for Numerical Simulation Software in Engineering and Sciences, Department of Engineering Mechanics, Hohai University, Nanjing* 210098*, China*)

Received 16 September 2008; revision received 5 March 2009

ABSTRACT The boundary knot method (BKM) is a truly meshless boundary-type radial basis function (RBF) collocation scheme, where the general solution is employed instead of the fundamental solution to avoid the fictitious outside boundary of the physical domain of interest. In this study, the BKM is first used to calculate the free vibration of free and simply-supported thin plates. Compared with the analytical solution and ANSYS (a commercial FEM code) results, the present BKM is highly accurate and fast convergent.

KEY WORDS boundary knot method, radial basis function, meshless, eigenvalues, vibration

I. INTRODUCTION

Nowadays numerical simulation has been playing an important role in engineering and scienctific applications. And the dominant numerical techniques have long been of the mesh-based numerical methods, such as finite element method (FEM), finite volume method, finite difference method, and boundary element method etc. However, the high-quality mesh generation of high-dimensional complicated geometry and moving boundary is still computationally very expensive and challenging[1,2]. Much effort has been devoted to the developing of meshless methods to cure this problem. Literally, the methods of this type avoid the mesh generation. The smooth particle hydrodynamics method[3] is one of the pioneering meshless techniques, which was originally developed to solve difficult astrophysical problems. Inspired by the work, recently quite a few meshless methods have been reported in the literature, for example, element-free Galerkin method[4], reproducing kernel method[5], method of fundamental solution (MFS)[6], boundary collocation method[7], boundary node method[8], boundary knots method (BKM)[9], and radial basis function (RBF) based methods[10–12].

Among various meshless methods, the MFS and the BKM are the two boundary-type RBF-based methods, which do not employ the moving least square at all and instead use the one-dimensional distance variable irrespective of the dimensionality of the problems. Therefore, these two methods are independent of dimensionality and complexity of the geometry and have distinct merits including being truly inherent meshless, easy-to-program, mathematically very simple, highly accurate, and fast convergent. However, the MFS, which employs the singular fundamental solution, was not yet a popular numerical method because it involves a controversial artificial boundary outside the physical domain. In general, the fictitious boundary is difficult to choose for a high-dimensional complicated geometry. This weakens the efficiency of the MFS to practical engineering problems[13,14]. The BKM, an improved

* Corresponding author. Email: chenwen@hhu.edu.cn

** Project supported by the National Natural Science Foundation of China (No.10672051).

approach, employs non-singular general solution instead of singular fundamental solution to evaluate the homogenous solution, and removes the controversial artificial boundary in the MFS. Some preliminary numerical experiments[15] show that the BKM can produce excellent results with a relatively small number of knots for various differential equation problems. However, the tested cases are mostly the second order systems.

Kang[16,17] and Chen[18–20] used the BKM to find the eigensolutions of free vibration membranes and plates with clamped boundary, and Kang[21] applies this method to the free vibration of membranes with cavity. However, the BKM has not be tested with free vibration plates of arbitrary shapes with complex and high order boundary conditions. In this study, the BKM is first employed to simulate the transverse vibration of arbitrary shaped plates subjected to free and simply-supported boundary conditions.

The remainder of this paper is organized as follows. §II introduces the governing equation of a free vibrating thin plate, the boundary conditions and the discretization method. §III presents some numerical examples, and compares the results with the analytical solution or ANSYS results. Based on the results reported here, §IV concludes this paper with remarks.

II. GOVERNING EQUATION OF FREE VIBRATION OF PLATES AND BOUNDARY CONDITIONS

2.1. Governing Equation of Free Vibration Plate

The governing equation for a free flexural vibration of a uniform thin plate can be expressed as

$$\nabla^4 w + \bar{m}\frac{\partial^2 w}{\partial t^2} = 0 \tag{1}$$

where $w = w(\boldsymbol{r}, t)$ is the transverse deflection, $\bar{m}$ is the surface density, t represents the time, D is the flexural rigidity expressed as $D = Eh^3/[12(1-\nu^2)]$ in terms of Young's modulus E, the Poisson's ratio ν and the plate thickness h. Assuming harmonic motion $w(\boldsymbol{r}, t) = \mathrm{e}^{\mathrm{i}\omega t}W(\boldsymbol{r})$, in which ω denotes the circular frequency and $W(\boldsymbol{r})$ represents the function of vibration mode, Eq.(1) can be rewritten as

$$\nabla^4 W - k^4 W = 0 \tag{2}$$

where

$$k = \sqrt[4]{\frac{\bar{m}\omega^2}{D}} \tag{3}$$

is the frequency parameter of the thin plate.

The zero-order 2D non-singular general solution of Eq.(2) is known as

$$W(\boldsymbol{r}) = J_0(k\boldsymbol{r}) + I_0(k\boldsymbol{r}) \tag{4}$$

where $J_0(\boldsymbol{r})$, $I_0(\boldsymbol{r})$ represent the zero-order Bessel and modified Bessel functions of the first kind, $\boldsymbol{r}$ is the Euclidean distance of the domain knots, respectively.

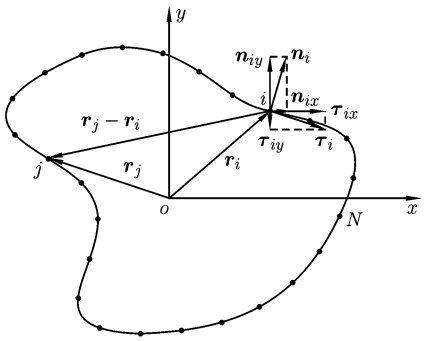

Fig. 1. The geometry configuration of an arbitrary shaped plate with N boundary knots distributed along the contour, $\boldsymbol{n}_{ix}$, $\boldsymbol{n}_{iy}$, $\boldsymbol{\tau}_{ix}$, $\boldsymbol{\tau}_{iy}$ are the horizontal and vertical components corresponding to the normal and tangential vectors $\boldsymbol{n}_i$, $\boldsymbol{\tau}_i$ of the ith knot, respectively.

Dividing the boundary into N installments and discretizing the zero-order general solution on the boundary, the vibration mode of the ith boundary knot is then determined by the sum of all the vibration modes relating to the ith knot (see Fig.1).

$$W(\boldsymbol{r}_i) = \sum_{j=1}^{N} \left[A_j J_0(k|\boldsymbol{r}_i - \boldsymbol{r}_j|) + B_j I_0(k|\boldsymbol{r}_i - \boldsymbol{r}_j|)\right] \qquad (i, j = 1, 2, \cdots, N) \tag{5}$$

where A_j and B_j are unknown coefficients.

2.2. Boundary Conditions

There are the following five boundary conditions of a vibrating plate to be encountered in this study. The displacement boundary condition is stated as

$$\boldsymbol{U} = W(\boldsymbol{r}) = \boldsymbol{0} \tag{6}$$

The slope along the normal direction on the boundary is

$$\boldsymbol{\theta} = \frac{\partial W(\boldsymbol{r})}{\partial \boldsymbol{n}} = \boldsymbol{0} \tag{7}$$

The bending moment condition on the boundary is

$$\boldsymbol{M} = \frac{\partial^2 W(\boldsymbol{r})}{\partial \boldsymbol{n}^2} + \nu \frac{\partial^2 W(\boldsymbol{r})}{\partial \boldsymbol{\tau}^2} = \boldsymbol{0} \tag{8}$$

The effective shear force on the free edges which parallel to the z-axis is

$$\boldsymbol{V} = \frac{\partial^3}{\partial \boldsymbol{n}^3} W(\boldsymbol{r}) + (2-\nu) \frac{\partial^3 W(\boldsymbol{r})}{\partial \boldsymbol{\tau}^2 \partial \boldsymbol{n}} = \boldsymbol{0} \tag{9}$$

The concentrated force at the polygonal corners of free edges is

$$\boldsymbol{R} = \frac{\partial^2 W(\boldsymbol{r})}{\partial \boldsymbol{n} \partial \boldsymbol{\tau}} = \boldsymbol{0} \tag{10}$$

where $\boldsymbol{n}, \boldsymbol{\tau}$ represent the outer normal and tangential direction of boundary knots, respectively. Equation (10) is the free corner boundary condition in which the two free edge encounter.

The BKM approximate solution representation in Eq.(5) is forced to satisfy the boundary displacement, slope, moment, shear force and free corner conditions, and then we get the following discretization equations:

$$W(\boldsymbol{r}_i) = \sum_{j=1}^{N} \left[A_j J_0(kr_{ij}) + B_j I_0(kr_{ij})\right] = \sum_{j=1}^{N} \left[A_j \boldsymbol{U}^J + B_j \boldsymbol{U}^I\right] = 0 \tag{11}$$

$$\frac{\partial W(\boldsymbol{r}_i)}{\partial \boldsymbol{n}_i} = \sum_{j=1}^{N} \left[A_j \frac{\partial}{\partial \boldsymbol{n}_i} J_0(kr_{ij}) + B_j \frac{\partial}{\partial \boldsymbol{n}_i} I_0(kr_{ij})\right] = \sum_{j=1}^{N} \left[A_j \boldsymbol{\theta}^J + B_j \boldsymbol{\theta}^I\right] = 0 \tag{12}$$

$$\begin{aligned}\left(\frac{\partial^2}{\partial \boldsymbol{n}_i^2} + \nu \frac{\partial^2}{\partial \boldsymbol{\tau}_i^2}\right) W(\boldsymbol{r}_i) &= \sum_{j=1}^{N} \left[A_j \left(\frac{\partial^2}{\partial \boldsymbol{n}_i^2} + \nu \frac{\partial^2}{\partial \boldsymbol{\tau}_i^2}\right) J_0(kr_{ij}) + B_j \left(\frac{\partial^2}{\partial \boldsymbol{n}_i^2} + \nu \frac{\partial^2}{\partial \boldsymbol{\tau}_i^2}\right) I_0(kr_{ij})\right] \\ &= \sum_{j=1}^{N} \left[A_j \boldsymbol{M}^J + B_j \boldsymbol{M}^I\right] = 0\end{aligned} \tag{13}$$

$$\begin{aligned}\left[\frac{\partial^3}{\partial \boldsymbol{n}_i^3} + \frac{(2-\nu)\partial^3}{\partial \boldsymbol{\tau}_i^2 \partial \boldsymbol{n}_i}\right] W(\boldsymbol{r}_i) &= \sum_{j=1}^{N} \left\{A_j \left[\frac{\partial^3}{\partial \boldsymbol{n}_i^3} + \frac{(2-\nu)\partial^3}{\partial \boldsymbol{\tau}_i^2 \partial \boldsymbol{n}_i}\right] J_0(kr_{ij}) + B_j \left[\frac{\partial^3}{\partial \boldsymbol{n}_i^3} + \frac{(2-\nu)\partial^3}{\partial \boldsymbol{\tau}_i^2 \partial \boldsymbol{n}_i}\right] I_0(kr_{ij})\right\} \\ &= \sum_{j=1}^{N} \left[A_j \boldsymbol{V}^J + B_j \boldsymbol{V}^I\right] = 0\end{aligned} \tag{14}$$

$$\begin{aligned}\frac{\partial^2 W(\boldsymbol{r}_i)}{\partial \boldsymbol{n}_i \partial \boldsymbol{\tau}_i} &= \sum_{j=1}^{N} \left[A_j \frac{\partial^2}{\partial \boldsymbol{n}_i \partial \boldsymbol{\tau}_i} J_0(kr_{ij}) + B_j \frac{\partial^2}{\partial \boldsymbol{n}_i \partial \boldsymbol{\tau}_i} I_0(kr_{ij})\right] \\ &= \sum_{j=1}^{N} \left[A_j \boldsymbol{R}^J + B_j \boldsymbol{R}^I\right] = 0\end{aligned} \tag{15}$$

where $r_{ij} = |\boldsymbol{r}_i - \boldsymbol{r}_j|$, $\boldsymbol{n}_i$, $\boldsymbol{\tau}_i$ respectively represent the outer normal and tangential vectors of the ith boundary knot shown as Fig.1, $(i = 1, 2, \cdots, N)$.

For simplicity, Eqs.(11-15) can be rewritten in matrix form as shown below:

$$\begin{bmatrix} \boldsymbol{U}^J & \boldsymbol{U}^I \\ \boldsymbol{\theta}^J & \boldsymbol{\theta}^I \\ \boldsymbol{M}^J & \boldsymbol{M}^I \\ \boldsymbol{V}^J & \boldsymbol{V}^I \\ \boldsymbol{R}^J & \boldsymbol{R}^I \end{bmatrix} \begin{bmatrix} \boldsymbol{A} \\ \boldsymbol{B} \end{bmatrix} = \boldsymbol{0} \tag{16}$$

The expression of each item in the coefficient matrix of Eq.(16) can be easily derived with details given in the Appendix.

Without the loss of generality, consider arbitrary shaped plates with simply supported boundaries as an example. The boundary conditions of arbitrary shaped plates with simply supported boundaries can be expressed as

$$\boldsymbol{U}^J\boldsymbol{A} + \boldsymbol{U}^I\boldsymbol{B} = \boldsymbol{0}, \qquad \boldsymbol{M}^J\boldsymbol{A} + \boldsymbol{M}^I\boldsymbol{B} = \boldsymbol{0} \tag{17}$$

Since the coefficients $\boldsymbol{A}$ and $\boldsymbol{B}$ have non-trivial solutions, by transforming the first formula in Eq.(17), the coefficient $\boldsymbol{B}$ can be stated as

$$\boldsymbol{B} = -[\boldsymbol{U}^I]^{-1}\boldsymbol{U}^J\boldsymbol{A} \tag{18}$$

and then substituting Eq.(18) into the second formula in Eq.(17), we can reduce the influence matrix from $2N$ order to N order shown as follows:

$$\left[\boldsymbol{M}^J - \boldsymbol{M}^I[\boldsymbol{U}^I]^{-1}\boldsymbol{U}^J\right]\boldsymbol{A} = [\mathrm{SS}]\boldsymbol{A} = \boldsymbol{0} \tag{19}$$

where $[\mathrm{SS}] = \boldsymbol{M}^J - \boldsymbol{M}^I[\boldsymbol{U}^I]^{-1}\boldsymbol{U}^J$ represents the influence matrix of a simply supported plate.

Due to the existence of non-trivial solution of $[\boldsymbol{A}]$, the determinants of the influence matrix corresponding to the eigenvalues must be zeros, namely,

$$\det[\mathrm{SS}(k)] = 0 \tag{20}$$

The frequency parameter k of a simply supported plate can be obtained from Eq.(20) through the iterative computation, and then substituting k into Eq.(3) to gain the natural frequency. In the following paragraphs, [S-SSSF(k)] represents the influence matrix of the unit square plate with three simply supported boundaries and one the free boundary, [$\boldsymbol{A}$-SSSS(k)] denotes the influence matrix of arbitrary shaped plates with simply supported boundaries.

III. NUMERICAL RESULTS AND DISCUSSIONS

3.1. Arbitrary Shaped Simply Supported Plate

Figure 2(a) shows the configuration of an arbitrary shaped plate, where the boundary is divided into $4N$-4 nodes. Figure 2(b) illustrates the normal and tangential directions of boundary knots. The nor-

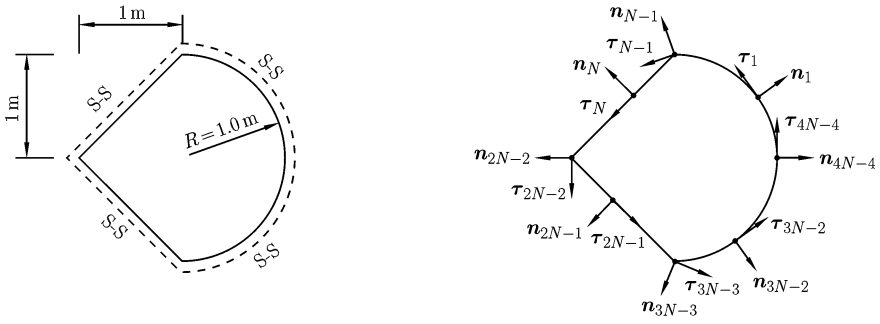

Fig. 2. (a) Geometry configuration of the arbitrary shaped plate, [S-S] denotes the simply supported edge. (b) The location of some discrete boundary knots and the corresponding normal and tangential directions, where each edge is divided into N installments, and $\boldsymbol{n}_i$, $\boldsymbol{\tau}_i$ denote the normal and tangential direction of the ith knot.

mal and tangential directions at polygonal corners are approximately determined by the sum of the two normal and tangential vectors at the adjacent edges respectively.

The eigenvalues of the simply supported plate shown as Fig.1(a) are given in the logarithm curve for $\det[\boldsymbol{A}\text{-SSSS}(k)] = 0$ shown as Fig.3. The troughs indicated by SK in the Fig.3 are the eigenvalues of the arbitrary shaped simply supported plate, and the crests indicated by MK are the eigenvalues of the corresponding shaped membrane which are actually spurious eigenvalues.

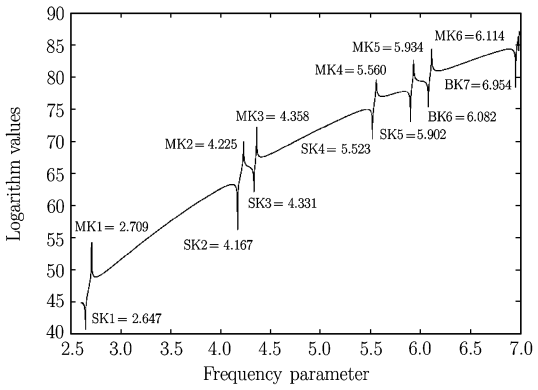

Fig. 3 Logarithm curves of the [$\boldsymbol{A}$-SSSS] plate with 20 ($N = 6$) boundary knots, $\nu = 0.3$, where SK denotes the frequency parameter of the [$\boldsymbol{A}$-SSSS] plate, and MK represents the frequency parameter of corresponding shaped membrane.

The reasons of the spurious eigenvalues may be that the $\partial^2 J_0(k\boldsymbol{r})/\partial \boldsymbol{n}^2$, $\partial^2 J_0(k\boldsymbol{r})/\partial \boldsymbol{\tau}^2$, $\partial^2 I_0(k\boldsymbol{r})/\partial \boldsymbol{n}^2$ and $\partial^2 I_0(k\boldsymbol{r})/\partial \boldsymbol{\tau}^2$ become singular at particular values of eigensolutions due to the fact that it is obtained via differentiating $J_0(k\boldsymbol{r})$, $I_0(k\boldsymbol{r})$ twice respectively to normal and tangential directions[16]. Therefore, the $2N \times 2N$ influence matrix of arbitrary simply supported plate must be reduced to $N \times N$ in order to eliminate the spurious eigenvalues of the corresponding shaped membrane in §2.2. However, this treatment will cause the influence matrix singular or close to singular.

It should be emphasized that it doesn't need to reduce the dimensions of the influence matrix of the square plate with simply supported edges since there is no spurious eigenvalues. However, we still cannot explain why this happens.

Table 1 displays the numerical eigenvalues of the arbitrary shaped simply supported plate (see Fig.2) obtained by BKM method and ANSYS FEM package. It is obvious that the numerical results obtained by the BKM agree well with the ANSYS solutions, and the highest relative discrepancy is less than 1.015%. Here ANSYS results serve as the comparative basis since the analytical solution of this case is not available.

Table 1. **Eigenvalues of the [$\boldsymbol{A}$-SSSS] plate obtained with the BKM**

Parameters	Present solutions				ANSYS	
	20 nodes (N=6)	Relative difference	24 nodes (N=7)	Relative difference	997 nodes	5419 nodes
SS1	2.647	1.015%	-	-	2.619	2.620
SS2	4.167	−0.091%	4.17	−0.019%	4.168	4.171
SS3	4.331	0.473%	4.332	0.496%	4.310	4.311
SS4	5.523	−0.087%	5.535	0.130%	5.523	5.528
SS5	5.902	0.075%	5.902	0.075%	5.895	5.898
SS6	6.082	0.012%	6.085	0.061%	6.079	6.081
SS7	6.954	−0.297%	6.971	−0.053%	6.967	6.975

'-' means that the influence matrix become too ill-conditioned to be calculated.

3.2. Cases with Mixed Boundary Conditions

A unit square plate with three simply supported boundaries and one free boundary [SSSF] is shown as Fig.4(a), whose boundary is divided into $4N$-4 installments. Here N is the knot number on each boundary. The location of some demonstrative knots and the corresponding normal directions are illustrated in Fig.4(b).

The eigenvalues of a unit square [SSSF] plate and a unit [SSSS] plate can be obtained from the logarithm curve of $\det[\text{S-SSSF}(k)] = 0$. The troughs indicated by [SF] in the Fig.5 are the eigenvalues of the unit square [SSSF] plate, and the crests indicated by [SS] are the eigenvalues of the corresponding shaped simply supported plate which are spurious eigenvalues in this case.

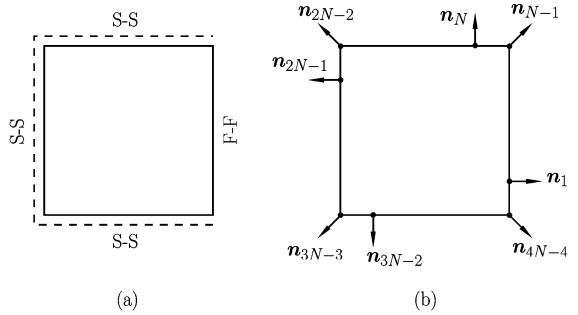

Fig. 4. (a) Geometry configuration of a unit square [SSSF] plate, [S-S] denotes the simply supported edge, [F-F] represents the free edge. (b) The location of some discrete boundary knots and the corresponding normal directions, $\boldsymbol{n}_i$ denotes the normal direction of the ith knot.

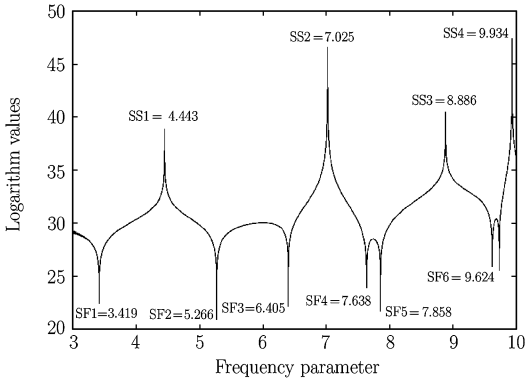

Fig. 5. Logarithm curves of the unit square [SSSF] plate with 20 ($N = 6$) boundary knots, $\nu = 0.3$, [SF] denotes the frequency parameter of the unit square [SSSF] plate; [SS] represents the frequency parameter of unit square simply supported plate.

Tables 2 and 3 respectively display the numerical and analytical eigenvalues of the unit square simply supported and [SSSF] plates. It is observed that the numerical solutions agree well with the analytical solution. It means that this numerical scheme produces very accurate solutions with small number of boundary knots. It should be mentioned that as the increase of frequency parameters, more boundary knots are required to get accurate solutions.

Table 2. **Eigenvalues of the unit [SSSS] square plate obtained with the BKM**

Parameters	Present solutions						Analytical Solution[22]
	20 nodes ($N = 6$)	Relative Error	24 nodes ($N = 7$)	Relative Error	28 nodes ($N = 8$)	Relative Error	
SS1	4.443	0.000%	-	-	-	-	4.443
SS2	7.025	0.000%	7.025	0.000%	7.025	0.000%	7.025
SS3	8.886	0.000%	8.886	0.000%	8.886	0.000%	8.886
SS4	9.934	−0.006%	9.935	0.000%	9.935	0.000%	9.935

Table 3. **Eigenvalues of the [SSSF] square plate obtained with the BKM**

Parameters	Present solutions						Analytical Solution[22]
	20 nodes ($N = 6$)	Relative Error	24 nodes ($N = 7$)	Relative Error	28 nodes ($N = 8$)	Relative Error	
SF1	3.419	0.029%	-	-	-	-	3.418
SF2	5.266	−0.040%	5.269	0.019%	-	-	5.268
SF3	6.405	−0.218%	6.421	0.031%	-	-	6.419
SF4	7.638	−0.618%	7.671	−0.182%	7.686	0.016%	7.685
SF5	7.858	−0.089%	7.866	0.013%	7.865	0.003%	7.865
SF6	9.624	1.279%	9.415	−0.916%	9.533	0.326%	9.502

IV. CONCLUSIONS

This paper tested the BKM to the free vibration plates of complex shape subjected to different boundary conditions. The numerical solutions are observed to agree well with the analytical solutions or the ANSYS FEM solutions. The BKM is found to be a simple but useful scheme[23] to simulate the free vibration problems.

One of the major findings in this study is that the method proposed by Kang[16,17] in calculating the eigenvalues of plates by reducing the influence matrix from dimension $2N\times 2N$ to $N\times N$ is not always efficient and its influence matrix may become singular or close to singular. Moreover, the accuracy of the BKM deteriorates in the solution of the simply-supported plate. We find that the culprit??? is the approach[16] to implement derivative boundary conditions at polygonal corners, in which the normal direction at polygonal corners of the plate is approximately determined by the sum of the two normal vectors for the adjacent edges. This study finds that this drawback can be easily remedied to guarantee the unit modal value of the normal vector.

On the other hand, it is noted that the present BKM scheme is not computationally cheap. Thus, the fast multipole method (FMM)[24], which has been developed to handle full matrix coefficient matrix as in the BKM case, can be employed to significantly improve the computational efficiency. The fast BKM is a subject currently under study and will be reported in a subsequent report.

Acknowledgement The authors are highly grateful to Wei Yang, a graduate student, for his assistance in this research.

References

[1] Zhang,Z., Gil,A.J., Hassan,O. and Morgan,K., The simulation of 3D unsteady incompressible flows with moving boundaries on unstructured meshes. *Computers & Fluids*, 2008, 37: 620-631.

[2] Bodard,N., Bouffanais,R. and Deville,M., Solution of moving-boundary problems by the spectral element method. *Applied Numerical Mathematics*, 2008, 58: 968-984.

[3] Krysl,P. and Belytschko,T., The element free Galerkin method for dynamic propagation of arbitrary 3D cracks. *International Journal for Numerical Methods in Engineering*, 1999, 44: 767-800.

[4] Lancaster,P. and Salkauskas,K., Surfaces generated by moving least-squares methods. *Mathematics of Computation*, 1981, 37: 141-158.

[5] Liu,W.K., Jun,S., Li,S., Adee,J. and Belyschko,T., Reproducing kernel particle methods for structural dynamics. *International Journal for Numerical Methods in Engineering*, 1995, 38: 1655-1679.

[6] Golberg,M.A. and Chen,C.S., The method of fundamental solutions for potential, Helmholtz and diffusion problems. In: Boundary Integral Methods: Numerical and Mathematical Aspects. Southampton: Computational Mechanics Publications, 1998, 103-176.

[7] Lothar,R., On the numerical solution of some 2-D electromagnetic interface problems by the boundary collocation method. *Computer Methods in Applied Mechanics and Engineering*, 1985, 53(1): 1-11.

[8] Mukherjee,Y.X. and Mukherjee,S., The boundary node method for potential problems. *International Journal for Numerical Methods in Engineering*, 1997, 40: 797-815.

[9] Chen,W., Symmetric boundary knot method. *Engineering Analysis with Boundary Elements*, 2002, 26(6): 489-494.

[10] Chen,C.S., Rashed,Y.F. and Golberg,M.A., A mesh-free method for linear diffusion equation. *Numerical Heat Transfer*, 1998, 33: 469-486.

[11] Golberg,M.A., Chen,C.S. and Ganesh,M., Particular solutions of 3D Helmholtz-type equations using compactly supported radial basis functions. *Engineering Analysis with Boundary Elements*, 2000, 24: 539-547.

[12] Zhang,X., Song,K.Z., Lu,M.W. and Liu,X., Meshless methods based on collocation with radial basis functions. *Computational Mechanics*, 2000, 26: 333-343.

[13] Kitagawa,T., Asymptotic stability of the fundamental solution method. *Journal of Applied Mathematics and Computing*, 1991, 38: 263-269.

[14] Balakrishnan,K. and Ramachandran,P.A., The method of fundamental solutions for linear diffusion-reaction equations. *Mathematical and Computer Modelling*, 2001, 31: 221-237.

[15] Hon,Y.C. and Chen,W., Boundary knot method for 2D and 3D Helmholtz and convection-diffusion problems under complicated geometry. *International Journal for Numerical Methods in Engineering*, 2003, 56: 1931-1948.

[16] Kang,S.W., Lee,J.M. and Kang,Y.J., Vibration analysis of arbitrarily shaped membranes using non-dimensional dynamic influence function. *Journal of Sound and Vibration*, 1999, 221: 117-132.

[17] Kang,S.W. and Lee,J.M., Free vibration analysis of arbitrary shaped plates with clamped edges using wave-type functions. *Journal of Sound and Vibration*, 2001, 241(1): 9-26.

[18] Chen,J.T., Chen,I.L., Chen,K.H., Lee,Y.T. and Yeh,Y.T., A meshless method for free vibration analysis of circular and rectangular clamped plates using radial basis function. *Engineering Analysis with Boundary Elements*, 2004, 28: 535-545.

[19] Chen,J.T., Chen,I.L., Chen,K.H. and Lee,Y.T., Comments on 'Free vibration analysis of arbitrarily shaped plates with clamped edges using wave-type functions'. *Journal of Sound and Vibration*, 2003, 262: 370-378.
[20] Chen,J.T., Chang,M.H., Chen,K.H. and Chen,I.L., The boundary collocation method with meshless concept for acoustic eigenanalysis of two-dimensional cavities using radial basis function. *Journal of Sound and Vibration*, 2002, 257(4): 667-711.
[21] Kang,S.W. and Lee,J.M., Application of free vibration analysis of membranes using the non-dimensional dynamic influence function. *Journal of Sound and Vibration*, 2000, 234(3): 455-470.
[22] Leissa,A.W., The free vibration of rectangular plates. *Journal of Sound and Vibration*, 1973, 3: 257-293.
[23] Laura,P.A.A. and Bambill,D.V., Comments on 'Free vibration analysis of arbitrarily shaped plates with clamped edges using wave-type functions'. *Journal of Sound and Vibration*, 2002, 252(1): 187-188.
[24] Rokhlin,V., Rapid solution of integral equations of classical potential theory. *Journal of Computational Physics*, 1985, 60: 187-207.

APPENDIX: DERIVATION OF MATRIX EQUATION (16)

The first normal directional derivative of the zero-order Bessel and modified Bessel function of the first kind are applied to clamped plates, and the detailed derivations are respectively shown as in expressions (21) and (22)

$$\frac{\partial}{\partial n_i}J_0(kr_{ij}) = -kJ_1(kr_{ij})(n_{ix}\cos\theta_{ij} + n_{iy}\sin\theta_{ij}) \tag{21}$$

$$\frac{\partial}{\partial n_i}I_0(kr_{ij}) = kI_1(kr_{ij})(n_{ix}\cos\theta_{ij} + n_{iy}\sin\theta_{ij}) \tag{22}$$

The second normal and tangential derivative of the zero-order Bessel and modified Bessel function of the first kind, which are used in simply free and supported plates, are deduced in Eqs.(23-26), respectively

$$\begin{aligned}\frac{\partial^2}{\partial n_i^2}J_0\left(kr_{ij}\right) &= -k^2J_0(kr_{ij})(n_{ix}\cos\theta_{ij} + n_{iy}\sin\theta_{ij})^2 \\ &\quad + \frac{k}{r}J_1(kr_{ij})\left(n_{ix}^2 - n_{iy}^2\right)\left(\cos^2\theta_{ij} - \sin^2\theta_{ij}\right)\end{aligned} \tag{23}$$

$$\begin{aligned}\frac{\partial^2}{\partial n_i^2}I_0\left(kr_{ij}\right) &= k^2I_0(kr_{ij})(n_{ix}\cos\theta_{ij} + n_{iy}\sin\theta_{ij})^2 \\ &\quad - \frac{k}{r}I_1(kr_{ij})\left(n_{ix}^2 - n_{iy}^2\right)\left(\cos^2\theta_{ij} - \sin^2\theta_{ij}\right)\end{aligned} \tag{24}$$

$$\begin{aligned}\frac{\partial^2}{\partial \tau_i^2}J_0\left(kr_{ij}\right) &= -k^2J_0(kr_{ij})(\tau_{ix}\cos\theta_{ij} + \tau_{iy}\sin\theta_{ij})^2 \\ &\quad + \frac{k}{r}J_1(kr_{ij})\left(\tau_{ix}^2 - \tau_{iy}^2\right)\left(\cos^2\theta_{ij} - \sin^2\theta_{ij}\right)\end{aligned} \tag{25}$$

$$\begin{aligned}\frac{\partial^2}{\partial \tau_i^2}I_0\left(kr_{ij}\right) &= k^2I_0(kr_{ij})(\tau_{ix}\cos\theta_{ij} + \tau_{iy}\sin\theta_{ij})^2 \\ &\quad - \frac{k}{r}I_1(kr_{ij})\left(\tau_{ix}^2 - \tau_{iy}^2\right)\left(\cos^2\theta_{ij} - \sin^2\theta_{ij}\right)\end{aligned} \tag{26}$$

The expressions in Eqs.(27-30) are the effective shear force on the free boundary; the detailed deductions are as follows:

$$\begin{aligned}\frac{\partial^3}{\partial n_i^3}J_0\left(kr_{ij}\right) &= \left[\left(k^3 - \frac{2k}{r^2}\right)J_1(kr_{ij}) + \frac{k^2}{r}J_0(kr_{ij})\right](n_{ix}\cos\theta_{ij} + n_{iy}\sin\theta_{ij})^3 \\ &\quad + \left[\frac{6k}{r^2}J_1(kr_{ij}) - \frac{3k^2}{r}J_0(kr_{ij})\right]\left(n_{ix}^3\sin\theta_{ij} + n_{iy}^3\cos\theta_{ij}\right)\sin\theta_{ij}\cos\theta_{ij}\end{aligned} \tag{27}$$

$$\begin{aligned}\frac{\partial^3}{\partial \tau_i^2\partial n_i}J_0\left(kr_{ij}\right) &= \left[\left(k^3 - \frac{2k}{r^2}\right)J_1(kr) + \frac{k^2}{r}J_0(kr)\right]\left(n_{ix}\tau_{ix}^2\cos^3\theta_{ij} + n_{iy}\tau_{iy}^2\sin^3\theta_{ij}\right) \\ &\quad + \left[\frac{6k}{r^2}J_1(kr) - \frac{3k^2}{r}J_0(kr)\right]\left(n_{ix}\tau_{ix}^2\sin\theta_{ij} + n_{iy}\tau_{iy}^2\cos\theta_{ij}\right)\cos\theta_{ij}\sin\theta_{ij}\end{aligned} \tag{28}$$

$$\frac{\partial^3}{\partial n_i^3} I_0\left(kr_{ij}\right) = \left[\left(k^3 + \frac{2k}{r^2}\right) I_1(kr_{ij}) - \frac{k^2}{r} I_0(kr_{ij})\right] (n_{ix}\cos\theta_{ij} + n_{iy}\sin\theta_{ij})^3 - \left[\frac{6k}{r^2} I_1(kr_{ij}) - \frac{3k^2}{r} I_0(kr_{ij})\right] \left(n_{ix}^3 \sin\theta_{ij} + n_{iy}^3 \cos\theta_{ij}\right) \sin\theta_{ij}\cos\theta_{ij} \tag{29}$$

$$\frac{\partial^3 I_0\left(kr_{ij}\right)}{\partial \tau_i^2 \partial n_i} = \left[\left(k^3 + \frac{2k}{r^2}\right) I_1(kr) - \frac{k^2}{r} I_0(kr)\right] \left(n_{ix}\tau_{ix}^2 \cos^3\theta_{ij} + n_{iy}\tau_{iy}^2 \sin^3\theta_{ij}\right) - \left[\frac{6k}{r^2} I_1(kr) - \frac{3k^2}{r} I_0(kr)\right] \left(n_{ix}\tau_{ix}^2 \sin\theta_{ij} + n_{iy}\tau_{iy}^2 \cos\theta_{ij}\right) \cos\theta_{ij}\sin^2\theta_{ij} \tag{30}$$

In expressions (21-30), n_{ix}, n_{iy} and τ_{ix}, τ_{iy}, respectively, represent the horizontal and vertical components, corresponding to the unit outer normal vector $n_i = n_{ix} + n_{iy}$ and the unit outer tangential vector $\tau_i = \tau_{ix} + \tau_{iy}$ defined at the ith boundary knot. θ_{ij} denotes the angle between the x-axis of Cartesian coordinate and the vector $(r_i - r_j)$.

However, some particular processes are required in the evaluation of $\cos\theta_{ij}$, $\sin\theta_{ij}$, $J_1(kr)$ and $I_1(kr)$, when the source and collocation points coincide each other. By using the L'Hôpital's rule, we find $\cos\theta_{ij} = \sin\theta_{ij} = 1/\sqrt{2}$ when $i = j$.

On the other hand, by using the mathematics symbol software, Maple, we reduce $J_1(kr)$ and $I_1(kr)$ as a series expansion:

$$J_1(kr) = \frac{1}{2}kr - \frac{1}{16}k^3r^3 + \frac{1}{384}k^5r^5 + O(r^6) \tag{31}$$

$$I_1(kr) = \frac{1}{2}kr + \frac{1}{16}k^3r^3 + \frac{1}{384}k^5r^5 + O(r^6) \tag{32}$$

In the practical calculation, the items $\frac{1}{16}k^3r^3$, $\frac{1}{384}k^5r^5$, $O(r^6)$ are both omitted when r approaches zero.